

IN-44  
22331  
13P

# InGaAs PV Device Development for TPV Power Systems

David M. Wilt  
*National Aeronautics and Space Administration  
Lewis Research Center  
Cleveland, Ohio*

Navid S. Fatemi and Richard W. Hoffman, Jr.  
*Essential Research, Inc.  
Cleveland, Ohio*

Phillip P. Jenkins and David Scheiman  
*NYMA, Inc.  
Engineering Services Division  
Brook Park, Ohio*

Roland Lowe  
*Kent State University  
Kent, Ohio*

Geoffrey A. Landis  
*NYMA, Inc.  
Engineering Services Division  
Brook Park, Ohio*

Prepared for the  
First Conference on Thermophotovoltaic Generation of Electricity  
sponsored by the National Renewable Energy Lab  
Copper Mountain, Colorado, July 24-26, 1994



National Aeronautics and  
Space Administration

N95-11587

Unclas

G3/44 0022331

(NASA-TM-106718) InGaAs PV DEVICE  
DEVELOPMENT FOR TPV POWER SYSTEMS  
(NASA. Lewis Research Center) 13 P



# InGaAs PV Device Development for TPV Power Systems

David M. Wilt, Navid S. Fatemi <sup>a)</sup>, Richard W. Hoffman, Jr. <sup>a)</sup>,  
Phillip P. Jenkins <sup>b)</sup>, David Scheiman<sup>b)</sup>, Roland Lowe <sup>c)</sup> and  
Geoffrey A. Landis <sup>b)</sup>

*NASA Lewis Research Center, Cleveland, Ohio 44135*

*<sup>a)</sup> Essential Research, Inc., Cleveland Ohio*

*<sup>b)</sup> NYMA, Inc., Brookpark, Ohio*

*<sup>c)</sup> Kent State University, Kent, Ohio*

**Abstract** Indium Gallium Arsenide (InGaAs) photovoltaic devices have been fabricated with bandgaps ranging from 0.75 eV to 0.60 eV on Indium Phosphide (InP) substrates. Reported efficiencies have been as high as 11.2% (AM0) for the lattice matched 0.75 eV devices. The 0.75 eV cell demonstrated 14.8% efficiency under a 1500°K blackbody with a projected efficiency of 29.3%. The lattice mismatched devices (0.66 and 0.60 eV) demonstrated measured efficiencies of 8% and 6% respectively under similar conditions. Low long wavelength response and high dark currents are responsible for the poor performance of the mismatched devices. Temperature coefficients have been measured and are presented for all of the bandgaps tested.

## INTRODUCTION

Research in thermophotovoltaic (TPV) power systems has persisted for many years, driven by high projected thermal to electric system efficiencies (ref. 1,2). Several variants of TPV systems have emerged with the principal difference being the method of thermal to radiant energy conversion. In blackbody based systems an emitter material is heated to produce broadband radiation. Unfortunately, much of the emitted energy is below the bandgap of the photovoltaic cell, therefore these systems must include some type of spectrum shaping element. This element must efficiently recycle the low energy photons back to the emitter in order to obtain high system efficiencies.

The other method of producing photons from thermal sources is based on selective emitters. These materials emit energy in a narrow spectral band when heated, eliminating the need for additional spectrum shaping elements. Chubb, et

al, have demonstrated rare earth doped Yttrium Alumina Garnets (YAG) crystals with good selective emission properties (ref. 3). Common to all TPV systems designed for operation at moderate temperatures ( $< 1500^{\circ}\text{K}$ ) is the need for a low bandgap photovoltaic device. For blackbody based systems, the optimum bandgap is dependant upon the operating temperature of both the emitter and the cell. For an emitter temperature of  $1500^{\circ}\text{K}$ , Woolf (ref. 2) has calculated that the optimum bandgap ranges from 0.52 eV to 0.82 eV depending upon the cell temperature. The optimum bandgap for selective emitter based systems depends upon the composition of the selective emitter (ref. 1).

The original work in TPV utilized standard silicon solar cells. The high bandgap of silicon ( $E_g = 1.1$  eV) limited the systems to very high emitter temperatures ( $> 2000^{\circ}\text{K}$ ). Radio-isotope and conventionally fueled heat sources operate at much lower temperatures, requiring lower bandgap photovoltaic devices. Indium Gallium Arsenide ( $\text{In}_x\text{Ga}_{1-x}\text{As}$ ) is a direct bandgap semiconductor material that has a bandgap ranging from 0.35 eV to 1.42 eV depending on the In/Ga ratio.  $\text{In}_{.53}\text{Ga}_{.47}\text{As}$  solar cells ( $E_g = 0.75$  eV), with efficiencies of up to 11.2% (AM0), have been fabricated on lattice matched indium phosphide (InP) substrates (ref. 4).

## EXPERIMENT

$\text{In}_x\text{Ga}_{1-x}\text{As}$  device structures were grown by Organo Metallic Vapor Phase Epitaxy (OMVPE) in a horizontal, low pressure reactor designed and constructed at NASA Lewis. The source gases consisted of trimethyl gallium, trimethyl indium, arsine (100%), phosphine (100%), diethyl zinc, and silane diluted in hydrogen. Typical growth conditions were:  $620^{\circ}\text{C}$  growth temperature, 190 torr reactor pressure, V/III ratio of 75, and carrier gas flow rate of 3.5 std. l/min. The InP substrates were zinc doped ( $p = 4 \times 10^{18} \text{ cm}^{-3}$ ), oriented (100) and used as received from the vendor. A co-flow of arsine and phosphine was used at the time of crossover from InP growth to InGaAs growth. The co-flow lasted 10 sec. and was used to protect the InP substrate from decomposition until the InGaAs had formed a continuous coverage. The growth rate of InP was  $6.1 \text{ \AA}/\text{sec}$  and the growth rate of InGaAs was  $8.1 \text{ \AA}/\text{sec}$ .

Device structures for the 0.75, 0.66 and 0.6 eV  $\text{In}_x\text{Ga}_{1-x}\text{As}$  devices are shown in figure 1. The lattice matched InGaAs device (0.75 eV) incorporated a very thick ( $1.5 \mu\text{m}$ ) InP window layer to reduce the series resistance. Modeling predicts a very high current density from this device ( $J_{sc} = 4.7 \text{ A}/\text{cm}^2$ ) under a  $1500^{\circ}\text{K}$  blackbody emitter (approximately equivalent to  $170 \times \text{AM0}$ ), therefore reduction of resistive losses through window layer design and front contact grid design will be very important. Losses due to absorption in the thick InP window layer are minimal under a  $1500^{\circ}\text{K}$  blackbody.

Lattice mismatched devices ( $E_g = 0.66$  and  $0.6$  eV) were also grown and incorporated step graded buffer layers between the InP substrate and the cell structure. These layers are intended to minimize the density of threading dislocations in the active device layers. An extensive examination of the effect of the grading structure on the performance of lattice mismatched devices is planned.

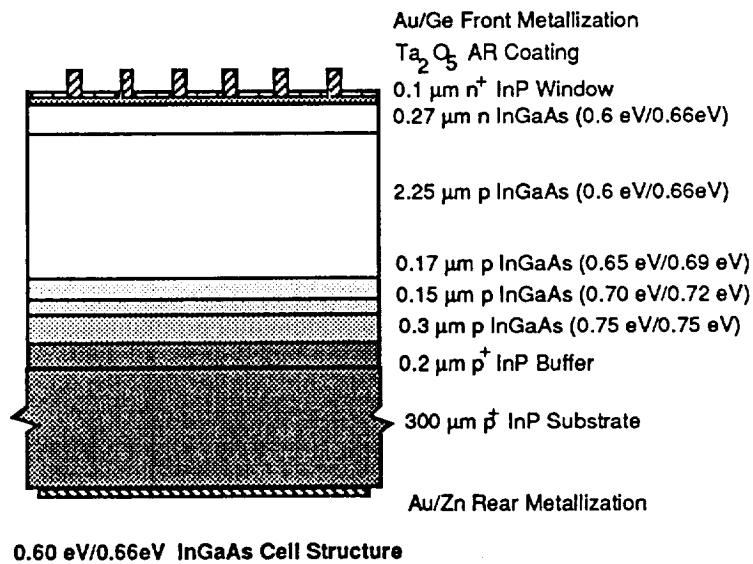
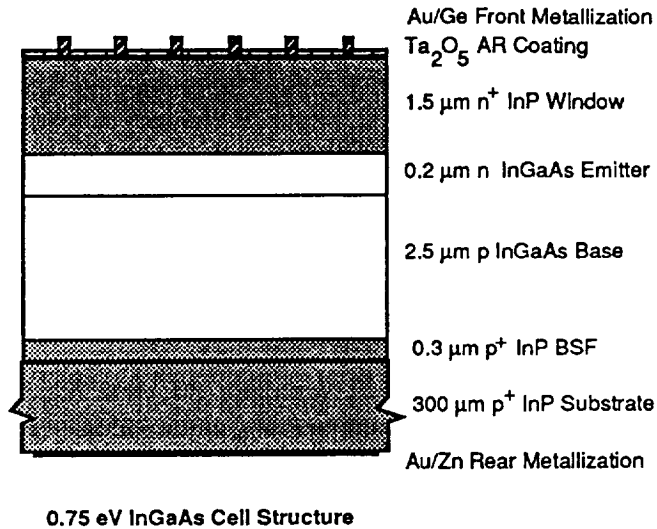


**Figure 1 - InGaAs TPV Cell Structures**

Due to the lattice mismatch (0.74% and 1.2%) of the 0.66 and the 0.6 eV material, thin InP window layers were used in these devices. Alternate window layer materials based on InAsP and AlInAs are under development to allow the incorporation of thick window layers for the reduction of series resistance.

The devices were processed using standard thermal evaporation and photolithographic techniques. The lattice mismatched cells were processed with a higher coverage front grid pattern to partially offset the limitations imposed by the high sheet resistance of the devices. Single layer anti-reflective coatings of  $\text{Ta}_2\text{O}_5$  were matched to the expected illumination source.

## RESULTS

Figure 2 shows the AM0 I-V data for the three different bandgap InGaAs devices without AR coatings. The large change in  $J_{sc}$  with bandgap is not directly related to bandgap, as might be thought. The 0.75 eV cell has a thick (1.5  $\mu\text{m}$ ) InP window layer that dramatically reduces the AM0  $J_{sc}$ , which can be seen in the external quantum efficiency (QE) data of figure 3. Dark diode measurements of the devices demonstrated that they were all diffusion limited, with diode ideality factors of  $\sim 1$ . The dark current showed a large dependence on lattice mismatch as can be seen in table 1.

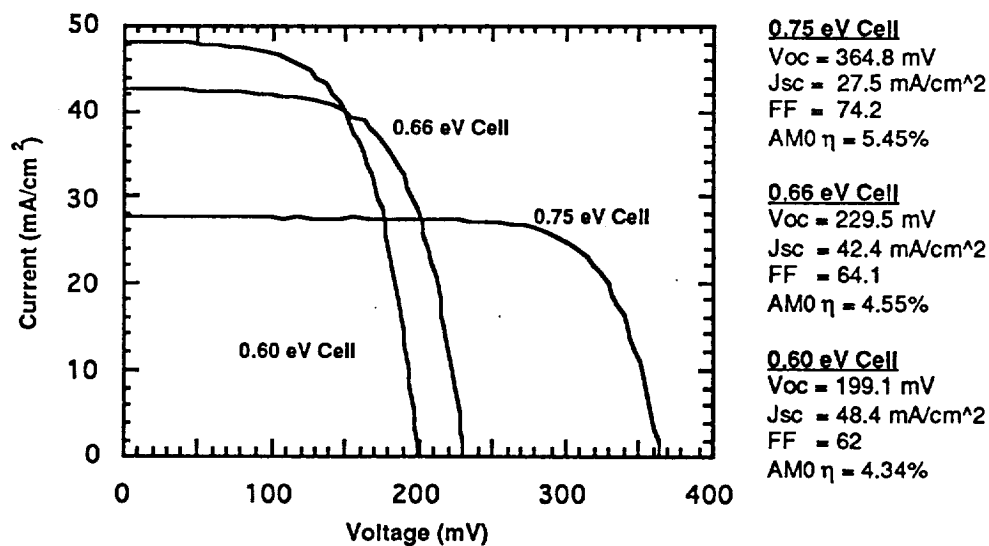


Figure 2. AM0 I-V data for InGaAs solar cells without AR coatings.

The external QE measurements (figure 3) were taken after  $\text{Ta}_2\text{O}_5$  AR coating deposition. Unfortunately, our equipment limits the measurements to 1.9  $\mu\text{m}$ , at which point the 0.6 and 0.66 eV cells are still operating. The roll off of the

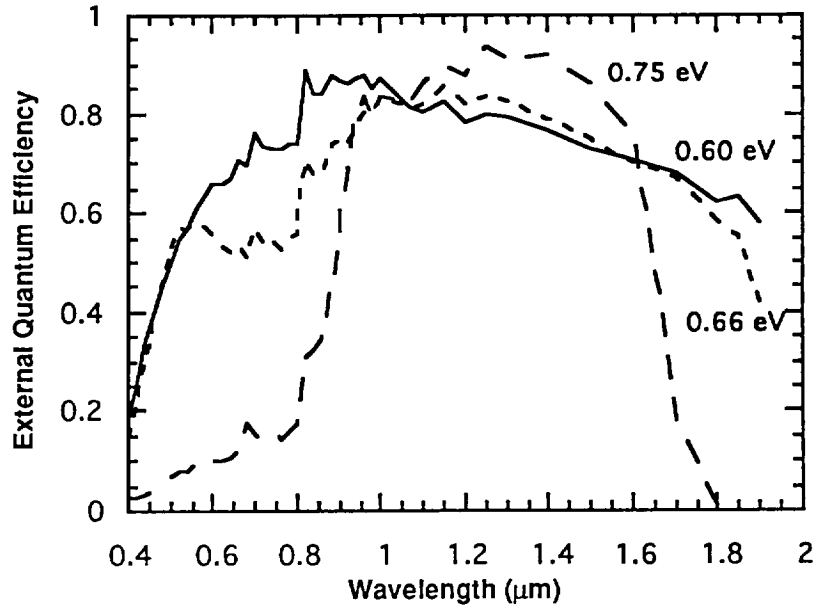


Figure 3. External QE measurements of AR Coated InGaAs Devices

mismatched InGaAs devices at the longer wavelengths is expected due to the deep absorption depth of the low energy photons and the short minority carrier lifetimes expected in the heavily dislocated material. Optimization of base thicknesses, doping levels and lattice grading structures should improve the long wavelength response.

The test devices were mounted on fixtures to facilitate their testing under blackbody and selective emitter illumination. The test fixture incorporated 4-wire connections for independent current and voltage measurement and a thermocouple mounted under the cell to monitor the operating temperature. An electric furnace, used for selective emitter development, was used as a 1500°K blackbody illumination source (fig. 4). Its' emissivity had previously been determined to be > 0.95. Calculations indicate that total emitted power from the black body should be 26.5 W/cm<sup>2</sup>, although measurements of the actual emitted power were only 3.0 W/cm<sup>2</sup> where the cells were mounted. This difference is attributed to the reduction in view factor which results from the 3.6 cm separating the cell from the furnace viewport.

The 0.75 eV cell was also measured under the illumination of an Er-YAG selective emitter at 1500°K (fig. 4). The measured output power from the selective emitter was 1.9 W/cm<sup>2</sup> at the cell test distance. This value is down from the 5.7 W/cm<sup>2</sup> value calculated from the measured selective emitter (SE) spectral

Bandgap (eV)	A	J01 (A/cm <sup>2</sup> )	Rs ( $\Omega$ )	Rsh ( $\Omega$ )
0.75	1.01	3.6e-8	0.453	3.4e3
0.66	0.99	6.5e-6	0.431	2.5e3
0.60	0.96	2.2e-5	0.387	8.0e2

Table 1. Dark diode data for InGaAs devices at 25 °C

emmissivity data. Difficulties were experienced in accurately determining the surface temperature of the SE and in keeping the entire exposed surface at a uniform temperature. Due to these errors we will not be reporting efficiencies for the InGaAs devices under SE illumination.

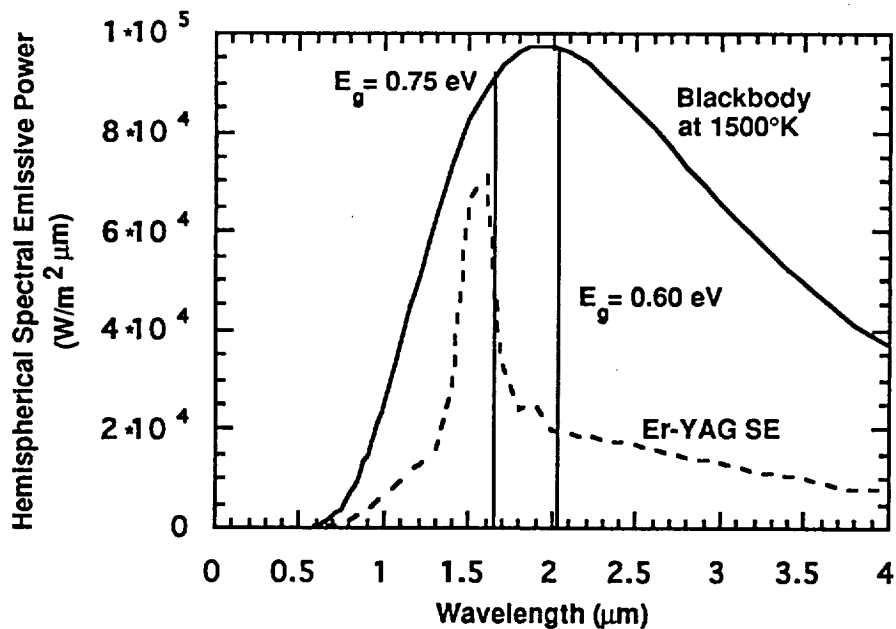


Figure 4. Blackbody and Er-YAG Selective Emitter Spectrum at 1500 °K.

The results of the test devices under the blackbody illumination are listed in table 2. As expected, the cell efficiency was very low without filters to reject the sub-bandgap photons from the incident spectrum. The 0.75eV cell is only able to absorb 16.8% of the total incident radiative energy. If the sub-bandgap portion of the spectrum is eliminated from the measurement, the incident power is reduced to 500 mW/cm<sup>2</sup> and the efficiency increases to 14.8%. An efficiency of 29.3% was predicted for this device. Those predictions assumed the illumination of the cell by a perfect black body (emissivity =1) at 1500°K with a view factor of 1, and used the measured SR and dark diode characteristics of the actual test device. The discrepancy in efficiencies is largely attributable to the low intensity of the actual

Bandgap (eV)	Measured Cell Efficiency w/o filter	Measured Cell Efficiency assuming a perfect filter	Calculated Cell Efficiency using Measured SR
0.75	2.5% #	14.8%	29.3%
0.66	1.9% #	8.0%	
0.60	1.9% #	6.0%	

# Cell Temperature = 34°C

Table 2 . Performance of InGaAs Devices under Blackbody Illumination

measurement compared to the calculated spectrum. The actual cell generated 277 mA/cm<sup>2</sup> of short circuit current, whereas the integration of the SR with the perfect blackbody spectrum predicted a J<sub>sc</sub> of 4.7 A/cm<sup>2</sup>. Achieving this optical coupling in actual practice will obviously entail the incorporation of optical concentrating elements, given the necessity of separating the emitter from the cell, for thermal management reasons.

Another reason for the large difference in the predicted vs. measured cell efficiency was a slight degradation in the cell performance after mounting on the test fixture. The cell had a lower shunt resistance after mounting, leading to a reduction in the fill factor. Additional experience in mounting devices should eliminate this problem. Calculated cell efficiencies for the 0.66 and 0.6 eV devices are not included due to the incomplete QE data for these devices.

Cell performance as a function of cell temperature is shown in figures 5-7 and table 3 under blackbody illumination. The temperature coefficients of V<sub>oc</sub> were very constant at -1.6 mV/°C for all of the bandgaps tested. As expected, the J<sub>sc</sub>

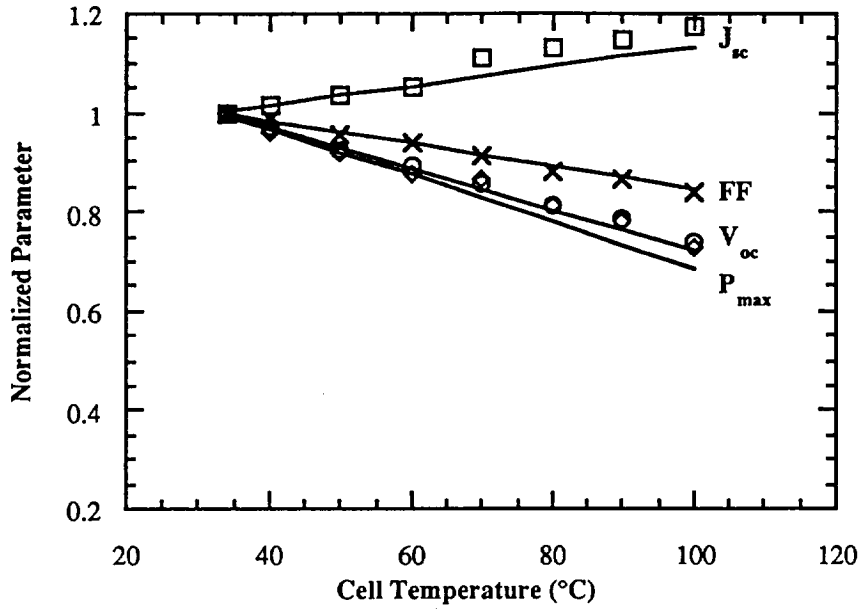


Figure 5. 0.75 eV InGaAs cell parameters vs. temperature under 1500°K blackbody illumination. Solid lines indicate curve fit to linear portion of data, between 30°C and 60°C.

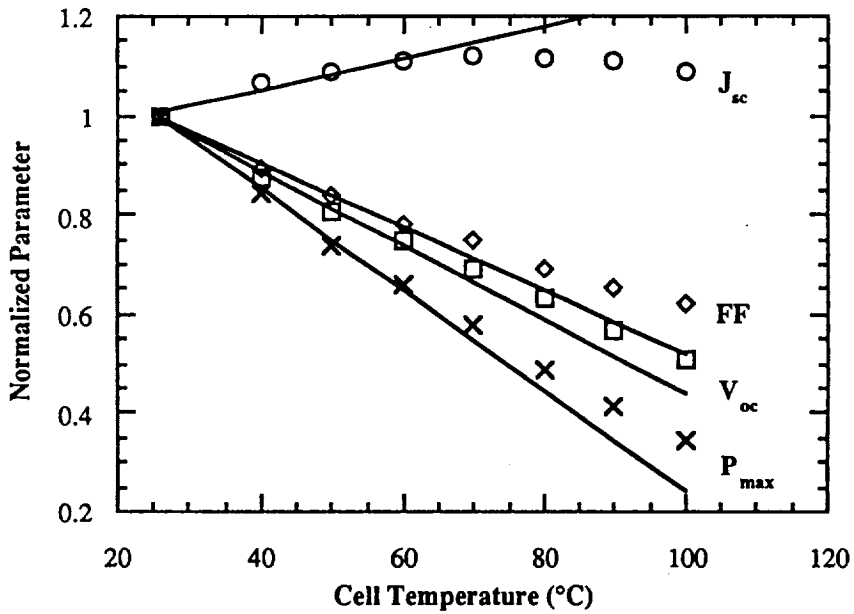


Figure 6. 0.66 eV InGaAs cell performance vs. temperature under 1500°K blackbody illumination. Straight lines indicate fits to the linear portion of the data, between 30°C and 60°C.

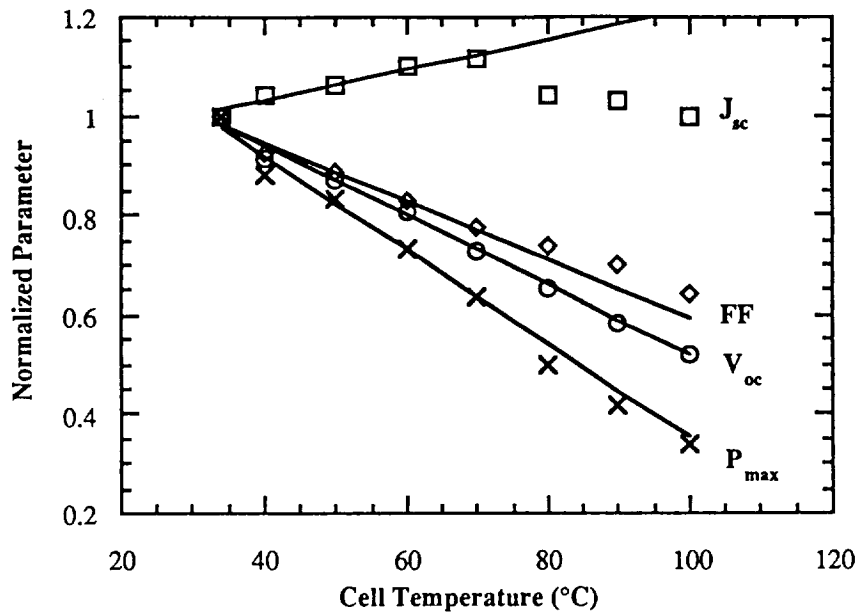


Figure 7. 0.60 eV InGaAs cell performance vs. temperature under 1500°K blackbody illumination. Straight line indicates fit to linear portion of data, between 30°C and 60 °C.

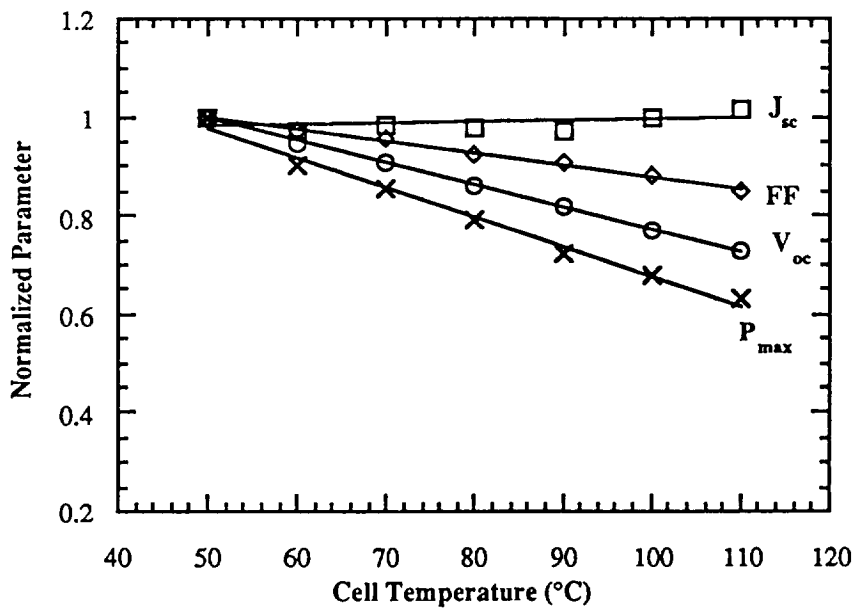


Figure 8. 0.75 eV InGaAs cell performance vs. temperature under Er-YAG selective emitter with a platinum substrate at ~1500°K.

increased with increasing cell temperature, due to bandgap narrowing. An interesting feature of the lattice mismatched devices is the peak in the  $J_{sc}$  at a cell temperature of  $\sim 70^\circ\text{C}$ . We believe that this is caused by increased recombination in the bulk as the temperature increases. The effect is more pronounced in the greater lattice mismatched 0.60 eV cell compared to the 0.66 eV cell. This indicates that the recombination mechanism may be related to the misfit and threading dislocations present in the mismatched InGaAs.

Bandgap (eV)	$(1/J_{sc})(dJ_{sc}/dT)$ ( $\times 10^{-3}/^\circ\text{C}$ )	$(1/V_{oc})(dV_{oc}/dT)$ ( $\times 10^{-3}/^\circ\text{C}$ )	$(1/FF)(dFF/dT)$ ( $\times 10^{-3}/^\circ\text{C}$ )	$(1/P_{max})(dP_{max}/dT)$ ( $\times 10^{-3}/^\circ\text{C}$ )	Linear Temperature Range ( $^\circ\text{C}$ )
0.75	1.99	4.20	2.32	4.67	30-60
0.66	3.18	7.44	6.39	1.01	30-60
0.60	3.04	6.97	5.87	9.46	30-70

Table 3 . Temperature Coefficients for InGaAs Cells Under 1500°K Blackbody Illumination

Figure 8 shows the temperature dependence for the 0.75 eV cell under the Er-YAG selective emitter. The small change in  $J_{sc}$  with increasing temperature indicates that the SE has very little emission outside of the Er related emission band.

## CONCLUSIONS

Lattice matched InGaAs has been demonstrated to have excellent potential for application in TPV power systems. Non-optimized device structures have projected efficiencies approaching 30% under 1500°K blackbody illumination. Lattice mismatched InGaAs devices offer the ability to “tune” the photovoltaic device response to correspond to the emission band of the illumination source. Results indicate that poor long wavelength response and high dark currents need to be addressed before these devices are feasible. Buffer layer design and dislocation passivation techniques are under development to improve device performance.

Modeling studies indicate that very high current densities can be expected from the photovoltaic devices in TPV systems. Minimizing the  $I^2R$  losses associated with these high currents requires the reduction of the series resistance. A novel window layer, based on aluminum indium arsenide, is under development

which will allow the incorporation of thick window layers, lattice matched to the mismatched InGaAs devices. In addition, a monolithically interconnected InGaAs array is being fabricated on a semi-insulating InP substrate to reduce the total current flowing through the structure. The semi-insulating InP substrate not only allows for device electrical isolation, it also has very low sub-bandgap free carrier absorption. This means that a back surface reflector can be incorporated which reflects low energy photons out of the device and hopefully back to the emission source. This should aide in maintaining reasonable cell operating temperatures and in improving the overall system efficiency.

## ACKNOWLEDGEMENT

The authors wish to acknowledge Auburn University - Space Power Institute for their support of this work under a cooperative Space Act Agreement. Auburn University has a grant from the U.S. Army Research Office for the development of TPV technology.

## REFERENCES

1. D. Chubb, R. Lowe and D. Flood, NASA TM 105755 (1992)
2. L.D. Woolf, Solar Cells **19**, 19 (1986).
3. R.L. Lowe, D.L. Chubb, S.C. Farmer and B.S. Good, "Rare Earth Garnet Selective Emitter", Appl. Phys. Lett. **64** (26). p. 3551 (1994)
4. D.M. Wilt, N.S. Fatemi, R.W. Hoffman, Jr., et al, Appl. Phys. Lett. **64** (18), p. 2415 (1994)

# REPORT DOCUMENTATION PAGE

Form Approved  
OMB No. 0704-0188

Public reporting burden for this collection of information is estimated to average 1 hour per response, including the time for reviewing instructions, searching existing data sources, gathering and maintaining the data needed, and completing and reviewing the collection of information. Send comments regarding this burden estimate or any other aspect of this collection of information, including suggestions for reducing this burden, to Washington Headquarters Services, Directorate for Information Operations and Reports, 1215 Jefferson Davis Highway, Suite 1204, Arlington, VA 22202-4302, and to the Office of Management and Budget, Paperwork Reduction Project (0704-0188), Washington, DC 20503.

<b>1. AGENCY USE ONLY (Leave blank)</b>	<b>2. REPORT DATE</b> August 1994	<b>3. REPORT TYPE AND DATES COVERED</b> Technical Memorandum	
<b>4. TITLE AND SUBTITLE</b>  InGaAs PV Device Development for TPV Power Systems		<b>5. FUNDING NUMBERS</b>  WU-233-01-0A	
<b>6. AUTHOR(S)</b>  David M. Wilt, Navid S. Fatemi, Richard W. Hoffman, Jr., Phillip P. Jenkins, David Scheiman, Roland Lowe, and Geoffrey A. Landis		<b>7. PERFORMING ORGANIZATION NAME(S) AND ADDRESS(ES)</b>  National Aeronautics and Space Administration Lewis Research Center Cleveland, Ohio 44135-3191	
<b>8. PERFORMING ORGANIZATION REPORT NUMBER</b>  E-9084		<b>9. SPONSORING/MONITORING AGENCY NAME(S) AND ADDRESS(ES)</b>  National Aeronautics and Space Administration Washington, D.C. 20546-0001	
<b>10. SPONSORING/MONITORING AGENCY REPORT NUMBER</b>  NASA TM-106718		<b>11. SUPPLEMENTARY NOTES</b>  Prepared for the First Conference on Thermophotovoltaic Generation of Electricity sponsored by the National Renewable Energy Lab, Copper Mountain, Colorado, July 24-26, 1994. David M. Wilt, NASA Lewis Research Center; Navid S. Fatemi and Richard W. Hoffman, Jr., Essential Research, Inc., 2460 Fairmont Blvd., Suite A, Cleveland, Ohio 44105 (work funded by NASA Contract NAS3-27243); Phillip P. Jenkins, David Scheiman, and Geoffrey A. Landis, NYMA, Inc., Engineering Services Division, 2001 Aerospace Parkway, Brook Park, Ohio 44142 (work funded by NASA Contract NAS3-27186); Roland Lowe, Kent State University, Kent, Ohio. Responsible person, David M. Wilt, organization code 5410, (216) 433-6293.	
<b>12a. DISTRIBUTION/AVAILABILITY STATEMENT</b>  Unclassified - Unlimited Subject Category 44		<b>12b. DISTRIBUTION CODE</b>	
<b>13. ABSTRACT (Maximum 200 words)</b>  Indium Gallium Arsenide (InGaAs) photovoltaic devices have been fabricated with bandgaps ranging from 0.75 eV to 0.60 eV on Indium Phosphide (InP) substrates. Reported efficiencies have been as high as 11.2% (AM0) for the lattice matched 0.75 eV devices. The 0.75 eV cell demonstrated 14.8% efficiency under a 1500°K blackbody with a projected efficiency of 29.3%. The lattice mismatched devices (0.66 and 0.60 eV) demonstrated measured efficiencies of 8% and 6% respectively under similar conditions. Low long wavelength response and high dark currents are responsible for the poor performance of the mismatched devices. Temperature coefficients have been measured and are presented for all of the bandgaps tested.			
<b>14. SUBJECT TERMS</b>  TPV; Thermophotovoltaics; InGaAs; Indium Gallium Arsenide; OMVPE; PV; Photovoltaics		<b>15. NUMBER OF PAGES</b> 13	
<b>17. SECURITY CLASSIFICATION OF REPORT</b> Unclassified		<b>16. PRICE CODE</b> A03	
<b>18. SECURITY CLASSIFICATION OF THIS PAGE</b> Unclassified	<b>19. SECURITY CLASSIFICATION OF ABSTRACT</b> Unclassified	<b>20. LIMITATION OF ABSTRACT</b>	